Nanoscale guiding for cold atoms based on surface plasmons along the tips of metallic wedges*

Wang Zheng-Ling(王正岭)[a)†], Tang Wei-Min(唐伟民)[a)], Zhou Ming(周 明)[b)c)], and Gao Chuan-Yu(高传玉)[b)]

[a)] *Department of Physics, Faculty of Science, Jiangsu University, Zhenjiang* 212013, *China*
[b)] *Center for Photon Manufacturing Science and Technology, School of Materials Science and Engineering, Jiangsu University, Zhenjiang* 212013, *China*
[c)] *State Key Laboratory of Tribology, Tsinghua University, Beijing* 100084, *China*

(Received 17 October 2012; revised manuscript received 4 February 2013)

We propose a novel scheme to guide neutral cold atoms in a nanoscale region based on surface plasmons (SPs) of one pair and two pairs of tips of metallic wedges with locally enhanced light intensity and sub-optical wavelength resolution. We analyze the near-field intensity distribution of the tip of the metallic wedge by the FDTD method, and study the total intensity as well as the total potential of optical potentials and van der Waals potentials for ^{87}Rb atoms in the light field of one pair and two pairs of tips of metallic wedges. It shows that the total potentials of one pair and two pairs of tips of metallic wedges can generate a gravito-optical trap and a dark closed trap for nanoscale guiding of neutral cold atoms. Guided atoms can be cooled with efficient intensity-gradient Sisyphus cooling by blue-detuned light field. This provides an important step towards the generation of hybrid systems consisting of isolated atoms and solid devices.

Keywords: nanoscale guiding, cold atoms, surface plasmons, metallic wedges

PACS: 37.10.Gh, 42.50.−p, 73.20.Mf, 78.67.−n **DOI:** 10.1088/1674-1056/22/7/073701

1. Introduction

In recent years, the laser guiding of neutral cold atoms has been widely applied in atomic optics as an important technique. For instance, the atomic guiding using a blue-detuned dark hollow mode,[1,2] a red-detuned Gaussian beam,[3,4] red-detuned Gaussian mode[5–7] or a blue-detuned evanescent wave[8] in the hollow optical fiber, TE_{01} doughnut mode in hollow metallic waveguides,[9] interference field composed of two hollow beams,[10] and so on. So far, neutral cold atoms have been successfully guided in a micron region, while schemes of nanoscale guiding of cold atoms have not been obtained due to the diffraction limit of light propagation.

More recently, the investigation of hybrid systems that integrate isolated atoms with solid devices has become a hot research subject in both atomic physics and nano-optics.[11–15] The crucial property of these devices is the ability of the designed system to trap and manipulate cold atoms near the surface of the device in a nanoscale region. To trap, guide, and manipulate cold atoms in a nanoscale region, several different methods have been proposed,[15–22] in which metallic nanometer structures have been paid more attention due to the property of plasmon resonances and exhibiting surface plasmons (SPs). In 2009, Chang *et al.* proposed a scheme to trap the isolated atoms using a paraboloid profile conductor nanotip,[15] while Murphy *et al.* proposed electro-optical nanotraps for neutral atoms.[19] In 2011, Stehle *et al.* demonstrated the coupling of plasmonic devices to single atoms by plasmonic micro- and submicrometer structures.[20]

Since the light field of the SPs can break the diffraction limit, the light field of SPs generated from the sub-wavelength metallic structure can be used to guide cold atoms in a nanoscale region. Because cold atoms are guided near the sub-wavelength metallic structure, the hybrid system integrating isolated atoms with solid devices can be formed, which can be used to study the coupling of plasmons and photons emitted from atoms. Therefore, it would be interesting and worthwhile to study and realize a novel atomic nanoscale guiding by using the sub-wavelength metallic structure. In this paper, we propose a novel scheme to generate nanoscale light fields for guiding neutral cold atoms by one pair and two pairs of tips of metallic wedges.

2. Guiding scheme and intensity analysis

A proposed scheme to generate a nanoscale light field to guide cold atoms is shown in Fig. 1. Figure 1(a) represents the scheme of the near field of a metallic wedge tip, Fig. 1(b) represents the scheme of the gravito-optical trap of a pair of tips of metallic wedges, and Fig. 1(c) represents the scheme of the dark nanoscale trap of two pairs of tips of metallic wedges. The section of the metallic wedge is a triangle with an end width L, and the perpendicular distance between the tip and end (that is the height of the triangle) is h. The coordinate sys-

*Project supported by the National Basic Research Program of China (Grant No. 2011CB013004), the National Natural Science Foundation of China (Grant No. 50975128), the Natural Science Foundation of Jiangsu Province, China (Grant No. BK2011462), and the Postdoctoral Science Foundation of China (Grant No. 20100481093).

†Corresponding author. E-mail: zlwang@ujs.edu.cn

© 2013 Chinese Physical Society and IOP Publishing Ltd

tem is set as shown in Fig. 1. In Fig. 1(a), the height of the triangle is along the y axis, and the tip line of the wedge is along the z axis. When the incident laser propagates from the medium onto the side of the metallic wedge, the near field of SPs with local enhanced distribution near the tip of a metallic wedge will be generated, in which the near field decreases almost exponentially from the maximum value at the tip with increasing distance from the tip (see Fig. 2).

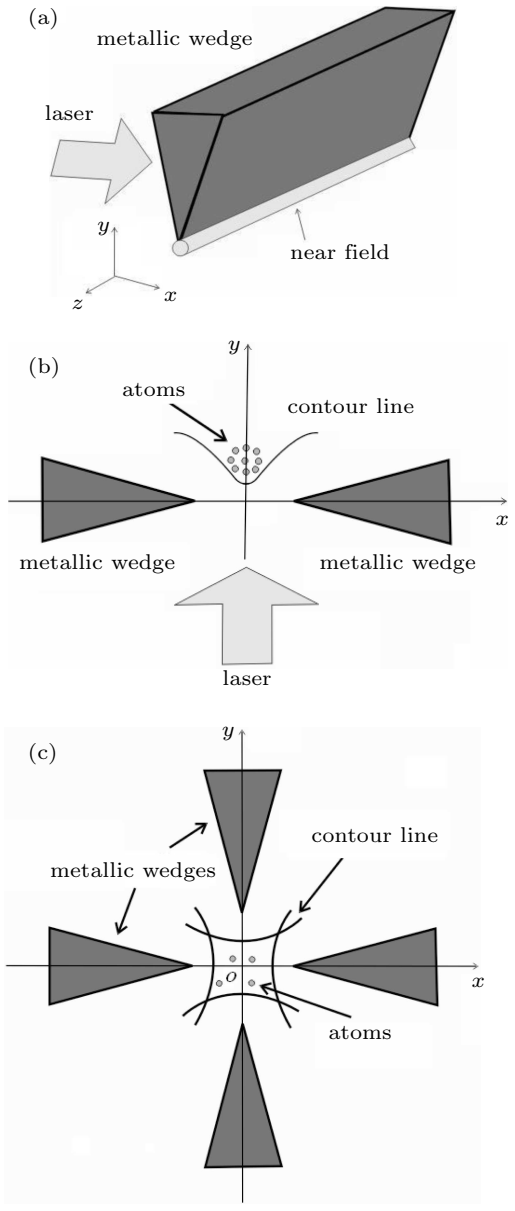


Fig. 1. Scheme diagram of the guiding of atoms in a nanoscale region. (a) Scheme of the near field of a metallic wedge tip; (b) scheme for gravito-optical trap of a pair of tips of metallic wedges; (c) scheme for the dark nanoscale trap of two pairs of tips of metallic wedges.

If near fields of one pair (or two pairs) of tips of metallic wedges are generated at the same time (see Fig. 1(b) or 1(c)), the nanoscale light section for guiding cold atoms will be constructed with blue detuning. To realize the loading of cold atoms, two-dimensional (2D) moving optical molasses are applied to prepare the MOT and generate a cold atomic beam above the center line (or along the propagating direction) of the center line of one pair (or two pairs) of tips of metallic wedges. Then, atoms can be transferred adiabatically to the blue-detuned light field and guided along it.[9]

By employing the finite-difference time-domain (FDTD) approach, we can derive the intensity distributions of the SPs near the tip of a metallic wedge or tips of a pair of metallic wedges, as shown in Figs. 2(a) and 2(b). Figure 2(a) shows contour lines of the intensity near the tip of a metallic wedge in the x–y plane. It can be observed from Fig. 2(a) that contour lines are approximately composed of a series of circles with the same center at the tip, and decreases from the maximum value at the tip with increasing distance from the tip. If the near-field distributions of one pair of metallic wedges (see Fig. 1(b)) are generated at the same time, the dark groove nanoscale light field will be constructed above the center. Contour lines of intensity of a pair of metallic wedges in the x–y plane are displayed in Fig. 2(b). Obviously, there is a grooved nanoscale light field above the center of a pair of metallic wedges, where cold neutral atoms will be moved to the lowest region of the groove by the gravity in the x–y plane and guided along the z axis, based on the blue-detuned light field. If the near-field distributions of two pairs of metallic wedges (as shown in Fig. 1(c)) are generated at the same time, the dark nanoscale light field will be constructed in the vicinity of the center. If the light field is blue-detuned, cold neutral atoms will be pushed to the vicinity of the center in the x–y plane and guided along the z axis.

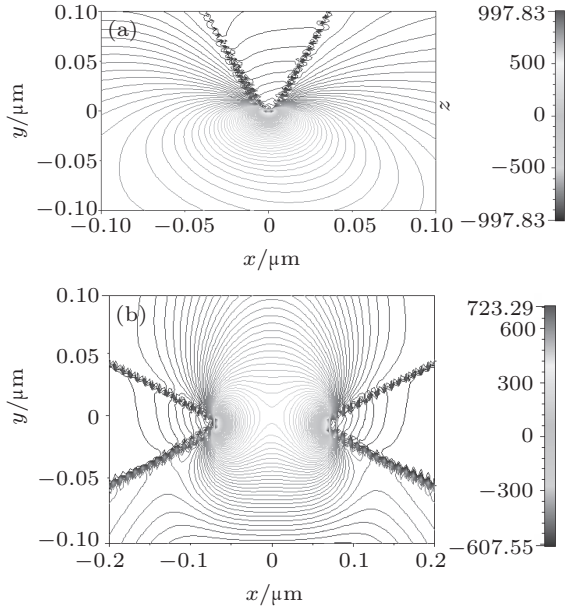


Fig. 2. Distribution of intensity in the x–y plane. (a) Contour lines of a wedge; (b) contour lines of a pair of wedges.

As we know, the FDTD approach depends on the direct numerical solution of the time-dependent Maxwell's curl equations and can obtain the very precise field distribution. Here, we consider 2D mode in the FDTD to simulate the field

distribution near the tip of the metallic wedge, i.e., the z direction in Fig. 1 is assumed to be infinite or the length of the metallic wedge is infinite. For the realistic case, if the metallic wedge is long enough to make the interesting guiding region much smaller than the length of the metallic wedge, 2D mode of the FDTD can be applied to simulate the field distribution near the tip of the metallic wedge and the corresponding error could be neglected. Therefore, we could use the optical intensity value calculated by the 2D simulation at a section plane to represent the value in the light field. In our simulation, the metallic wedge is made up of Ag, the medium is air, the end width $L = 0.4$ μm, the height of the triangle $h = 0.6$ μm, the tip is circular with a curvature radius of 5 nm, and the wavelength of the incident laser $\lambda = 0.78$ μm. Since the TE mode can only generate a very large light spot without the SPs, we take the TM mode to generate the SPs which can break the diffraction limit. In the case of a metallic wedge as shown in Fig. 1(a), we use an incident laser beam in the x direction, and the near field of SPs is shown in Fig. 2(a). In the case of a pair of metallic wedges as shown in Fig. 1(b), we use an upward incident laser beam, and the near field of SPs near two tips of metallic wedges will be added up, and then the dark groove nanoscale light section above the center of a pair of metallic wedges is generated, as shown in Fig. 2(b).

Figure 2(a) demonstrates that the maximal value of intensity is at the tip, that is, at the point $x = 0.0$ μm, $y = 0.0$ μm in Fig. 1(a). Due to local enhanced effect of the SPs, the maximal intensity at the tip can increase to 997.83 times of the incident intensity I_0. In Figs. 2–6, the intensity is in unit of I_0.

The distribution of the intensity in the vicinity of the tip in the x and y directions is discussed in detail (see Fig. 2(a) and Fig. 3). Figure 3(a) shows the dependence of intensity on y as $x = 0.0$ μm, where the difference in dependence of intensity between metal and medium can be found. In the metal, the intensity decreases steeply from the maximal value to 0 in a very short distance. While in the medium, the intensity decreases almost exponentially from the maximum value at the tip ($y = 0.0$ μm) to 93 times of I_0 at $y = -0.5$ μm. Similarly, Fig. 3(b) shows the dependence of intensity on x as $y = 0.0$ μm, in which the dependence of intensity on x is symmetric and the full width at half height of the intensity in the x direction is about 12.8 nm.

To study the intensity and optical potential more conveniently, from Fig. 3(a), we can obtain the analytic expression of the intensity distribution in the vicinity of the tip in the medium by the second order exponential fit as follows:

$$I(r)=I_0\left[294.52\exp\left(\frac{-r}{0.05}\right)+568.85\exp\left(\frac{-r}{0.0051}\right)+109.44\right], \quad (1)$$

where I_0 is the incident intensity, and r is the distance from the tip of the metallic wedge in the medium. According to Eq. (1), Figs. 3(a) and 3(b), we compare the intensity between the fitted result and simulation values. The straight line in Fig. 4 shows the dependence of the intensity on r in the vicinity of the tip in the medium from Eq. (1). The dotted line (simulation 1) in Fig. 4 shows the dependence of the intensity on r from the tip in the $-y$ direction by the simulation as shown in Fig. 3(a), and the dashed line (simulation 2) in Fig. 4 shows the dependence of the intensity on r from the tip in the x direction from the simulation as shown in Fig. 3(b). Since the dotted line in Fig. 4 is well consistent with the solid line and the dashed line in Fig. 4 is almost (the maximal relative error is 7.4%) consistent with the solid line, we can take Eq. (1) to study approximately the intensity and the optical potential of atoms guided in the nanoscale optical field.

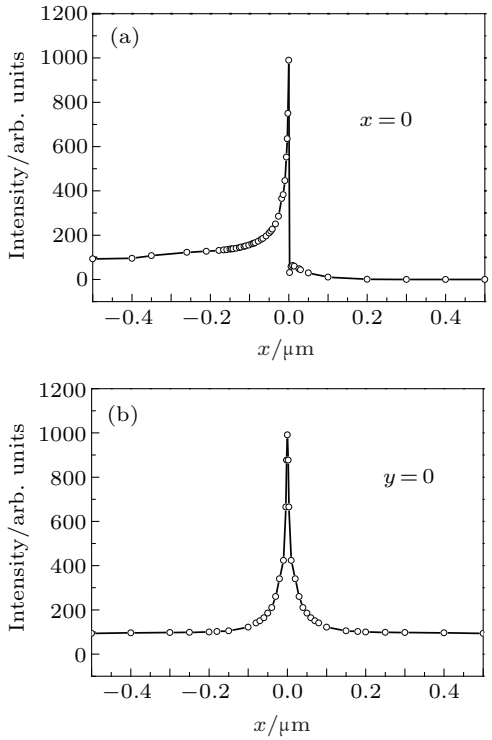


Fig. 3. Dependence of intensity (a) on the y axis as $x = 0.0$ μm; (b) on the x axis as $y = 0.0$ μm.

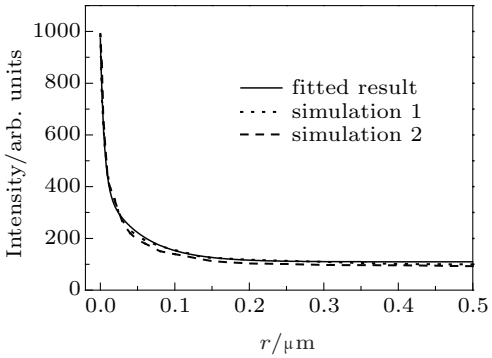


Fig. 4. Comparison of the dependence of intensity of a metallic wedge tip on r between the fitted result and simulation values.

In the scheme of one pair and two pairs of tips of metallic wedges in Figs. 1(b) and 1(c), the distance between the tip and 0 is set as d. Figure 5(a) shows the dependence of intensity of a metallic wedge tip on x as $y = 0.0$ μm, in which $-d_1$, $-d_2$,

$-d_3$, $-d_4$, and $-d_5$ represent only considering the left metallic wedge tip with a distance between the tip and 0 of 0.05, 0.1, 0.15, 0.2, and 0.25 μm, respectively, while d_1, d_2, d_3, d_4, and d_5 represent only considering the right metallic wedge tip with a distance between the tip and 0 of 0.05, 0.1, 0.15, 0.2, and 0.25 μm, respectively. Figure 5(b) shows the dependence of total intensity of a pair of metallic wedge tips (considering both the left and right metallic wedges) on x as $y = 0.0$ μm, in which d_1, d_2, d_3, d_4, and d_5 represent a distance between the tip and 0 of 0.05, 0.1, 0.15, 0.2, and 0.25 μm, respectively. That is to say, the distance between two tips is 0.1, 0.2, 0.3, 0.4, and 0.5 μm, respectively. Figure 5(b) demonstrates the distribution of total intensity of a pair of metallic wedge tips in the straight line between two tips, and shows that there is a minimum intensity in the center of a pair of metallic wedge tips.

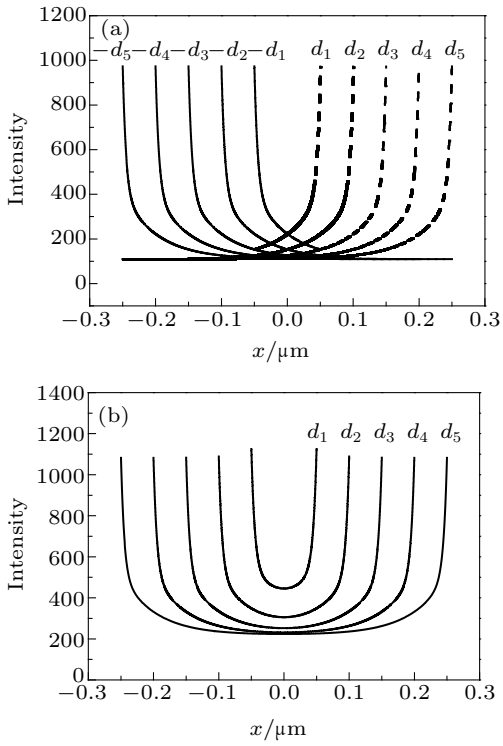


Fig. 5. (a) Dependence of intensity of a metallic wedge tip on x as $y = 0.0$ μm with different d ($-d$ represents the left metallic wedge tip only and d represents the right one only). Here, d is the distance between the tip and 0. (b) Dependence of intensity of a pair of metallic wedge tips on x as $y = 0.0$ μm with different d.

Figures 6(a) and 6(b) show the distribution of total intensity of a pair of metallic wedge tips in the x–y plane as $d = 0.075$ and 0.25 μm, respectively. Obviously, there is a grooved nanoscale light field above the center of a pair of metallic wedges, which is similar to the simulated result as shown in Fig. 2(b). Therefore, there is a gravito-optical trap for cold neutral atoms near the lowest region of the groove in the x–y plane of a pair of metallic wedge tips based on the blue-detuned light field. Figure 6(c) shows the distribution of total intensity of two pairs of metallic wedge tips in the x–y plane as $d = 0.25$ μm. Obviously, the dark light field will be constructed in the vicinity of the center, which indicates that two pairs of metallic wedges can generate a dark optical potential for cold atoms under the condition of blue-detuning and can realize the trapping of atoms in the vicinity of the center of two pairs of wedge tips.

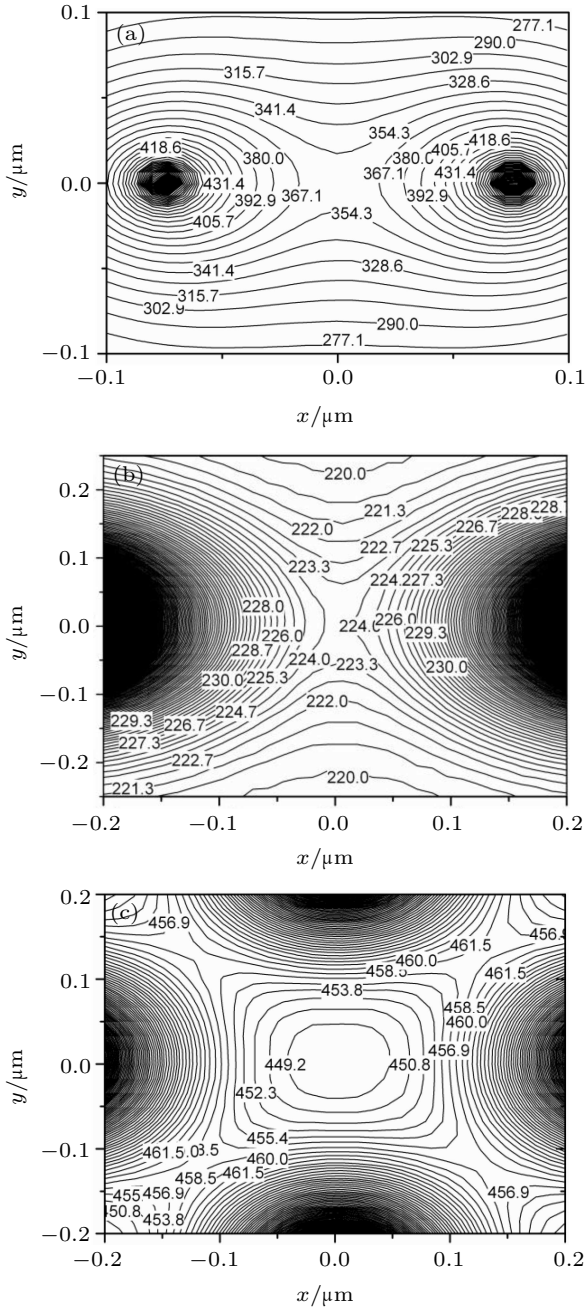


Fig. 6. Distribution of total intensity of a pair of metallic wedge tips in the x–y plane as (a) $d = 0.075$ μm and (b) $d = 0.25$ μm. (c) Distribution of total intensity of two pairs of metallic wedge tips in the x–y plane as $d = 0.25$ μm.

3. Potential analysis and intensity gradient cooling of atoms

Here, we choose the lower hyperfine ground state of the alkali-metal ^{87}Rb atom as the guided state. In view of the cou-

pling of the three-level ^{87}Rb atom with a blue-detuned light field, the expression of the optical potential of atoms in the lower hyperfine ground state can be given by[9,23]

$$U_{\rm opt} = -\frac{\hbar\delta}{2} + \frac{\hbar(\delta^2+\Omega^2)^{1/2}}{2}, \tag{2}$$

where $\delta/2\pi$ is the laser detuning from the atomic resonance frequency, $\Omega = \Gamma\sqrt{I/2I_{\rm sat}}$ represents the Rabi frequency, $I_{\rm sat}$ is the saturation intensity, Γ is the natural linewidth, and $I$is the light intensity given by Eq. (1). For ^{87}Rb-D_2 line atoms, $\Gamma/2\pi = 6$ MHz, and $I_{\rm sat} = 1.67$ mW/cm^2. In addition, atoms are not only pushed by the optical potential, but also attracted by the van der Waals attracting potential. For ^{87}Rb atoms near the tip of the Ag wedge, the van der Waals attracting potential can be approximately written in the simple form[15]

$$U_{\rm vdW} \approx -\frac{3}{32}\frac{\hbar\Gamma}{(kr)^3} \tag{3}$$

where $k = 2\pi/(0.78\times10^{-6})$ for ^{87}Rb atoms, and r is the distance from the tip of the metallic wedge to the atom in the medium. The total potential of atoms can be given by $U = U_{\rm opt} + U_{\rm vdW}$.

According to Eqs. (1)–(3), we calculate the distribution of 2D contour lines of total potential for ^{87}Rb atoms of one pair of metallic wedge tips in the x–y plane as $d = 0.075$ μm and $\delta/2\pi = 3.0$ GHz. Results for $I_0 = 2.5\times10^3$ W/m^2 and 5.0×10^3 W/m^2 are shown in Figs. 7(a) and 7(b), respectively. It is obvious from Fig. 7(a) that the van der Waals attracting potential plays an important role in the total potential for small d and I_0, and there is a maximum total potential at the center of one pair of tips of metallic wedges and there is no gravito-optical trap above the center of two tips. If we increase I_0 to 5.0×10^3 W/m^2, as shown in Fig. 7(b), we find that there is a groove of total potential above the center of one pair of tips of metallic wedges, and there is a gravito-optical trap above the center of two tips of metallic wedges. To decrease and eliminate the influence of the van der Waals attracting potential, we can increase d. Distributions of 2D contour lines of total potential for ^{87}Rb atoms of one pair of metallic wedge tips in the x–y plane as $d = 0.25$ μm, $\delta/2\pi = 3$ GHz, $I_0 = 2.0\times10^2$ W/m^2, and 1.0×10^3W/m^2 are shown in Figs. 7(c) and 7(d), respectively. We can see from Figs. 7(b)–7(d) that there is a groove total potential above the center of a pair of metallic wedge, and there is a gravito-optical trap for cold neutral atoms near the lowest region of the groove in the x–y plane based on the blue-detuned light field. The gravito-optical trap may trap nearly all atoms ($T = 120$ μK) released from the two-dimensional moving optical molasses (MOT) and guide them along the z axis in this gravito-optical trap.

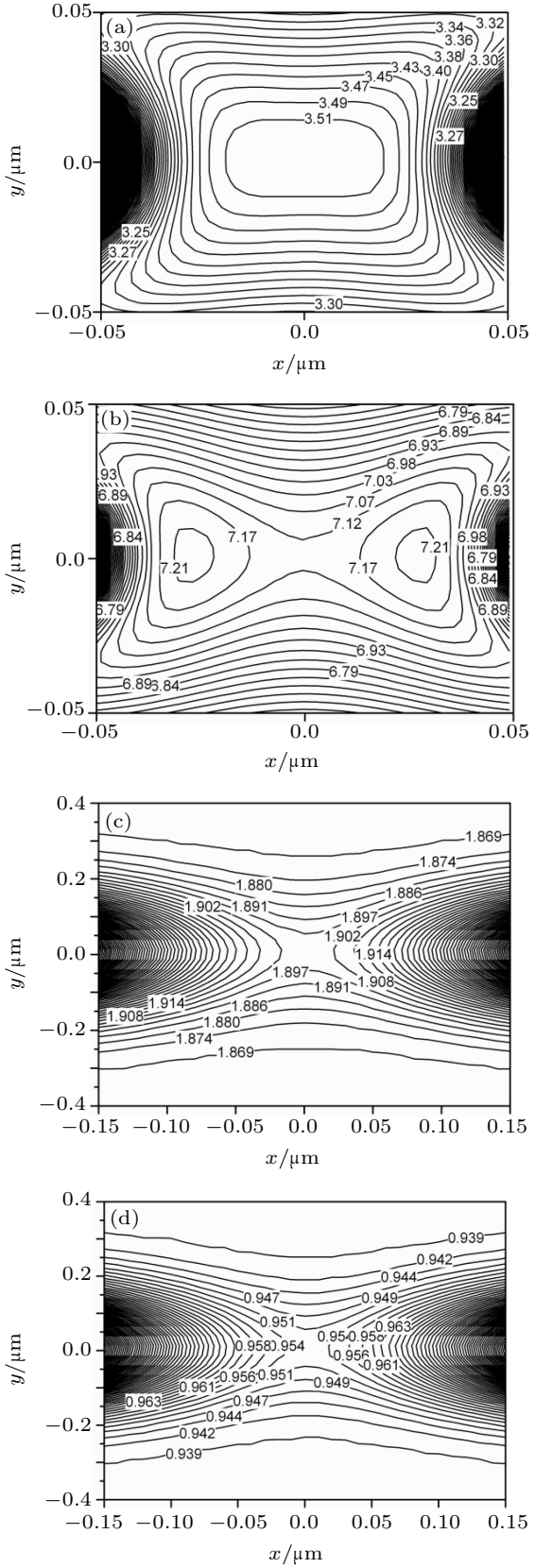


Fig. 7. Distribution of 2D contour lines of total potential for ^{87}Rb atoms of one pair of metallic wedge tips in the x–y plane as $\delta/2\pi = 3.0$ GHz, (a) $d = 0.075$ μm, $I_0 = 2.5\times10^3$ W/m^2; (b) $d = 0.075$ μm, $I_0 = 5.0\times10^3$ W/m^2; (c) $d = 0.25$ μm, $I_0 = 2.0\times10^2$ W/m^2; (d) $d = 0.25$ μm, $I_0 = 1.0\times10^3$ W/m^2. Here, the unit of potential is mK.

Similarly, according to Eqs. (1)–(3), we calculate the distribution of 2D contour lines of total potential for ^{87}Rb atoms

in the vicinity of the center of two pairs of metallic wedge tips in the x–y plane, as $d = 0.25$ μm, $I_0 = 1.0 \times 10^4$ W/m^2, and $\delta/2\pi = 3.0$ GHz, and the result is shown in Fig. 8. It is obvious from Fig. 8 that there is a minimum total potential at the center of two pairs of tips of metallic wedges. In addition, according to Eqs. (1) and (3), 1D distributions of total potential in the x direction and in the diagonal direction for ^{87}Rb atoms of two pairs of metallic wedge tips are calculated as $d = 0.25$ μm. Figure 9(a) shows the dependence of total potential on x for $I_0 = 1.0 \times 10^4$ W/m^2 and different $\delta/2\pi$. Figure 9(b) shows the dependence of total potential on x as $\delta/2\pi = 3.0$ GHz for different I_0. Figure 9(c) shows the dependence of total potential on t (the diagonal distance from 0 when $y = x$ or $y = -x$) as $I_0 = 1.0 \times 10^4$ W/m^2 for different $\delta/2\pi$. Figure 9(d) shows the dependence of total potential on t as $\delta/2\pi = 3.0$ GHz for different I_0. It is obvious from Fig. 9 that the total potential will increase with increasing I_0 for equal $\delta/2\pi$, and the total potential will increase with decreasing $\delta/2\pi$ for equal I_0.

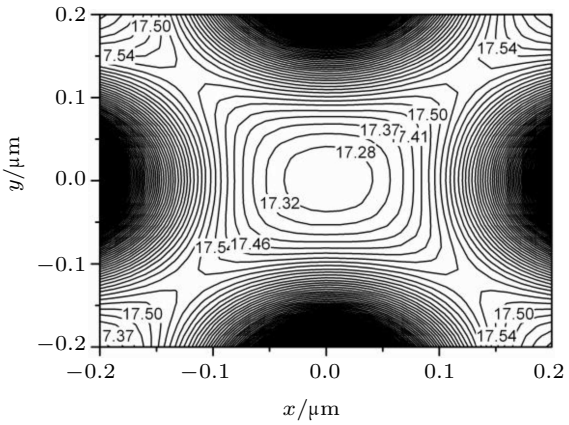


Fig. 8. 2D contour lines of total potential for ^{87}Rb atoms in the vicinity of the center of two pairs of metallic wedge tips in the x–y plane as $d = 0.25$ μm, $I_0 = 1.0 \times 10^4$ W/m^2, and $\delta/2\pi = 3.0$ GHz. Here, the unit of potential is mK.

Here, the interesting concept is the trapping depth of cold atoms, which is defined as the difference between the maximal total potential and the minimum total potential at the center in this dark nanoscale trap. We find from Figs. 8 and 9 that the trapping depth is maximal in the x and y directions and minimum in the diagonal direction. Therefore, the trapping depth of the system is determined by the trapping depth in the diagonal direction. According to Fig. 9(c), the trapping depth increases with decreasing $\delta/2\pi$ for the same I_0, and their values are 0.52, 0.42, 0.32, and 0.25 mK as $I_0 = 1.0 \times 10^4$ W/m^2 and $\delta/2\pi = 1.0$, 2.0, 3.0, and 4.0 GHz, respectively. We can also find from Fig. 9(d) that the trapping depth will increase with increasing I_0 for equal $\delta/2\pi$, and their values are 0.32, 0.46, 0.58, and 0.69 mK as $\delta/2\pi = 3.0$ GHz, and $I_0 = 1.0 \times 10^4$, 1.5×10^4, 2.0×10^4, and 2.5×10^4 W/m^2, respectively. These trapping depths may trap nearly all atoms ($T = 120$ μK) released from the two-dimensional moving optical molasses and then loaded into the dark nanoscale trap. In fact, atoms with a temperature of 120 μK are trapped in the region with a section diameter of about 134.0 nm as $I_0 = 1.0 \times 10^4$ W/m^2 and $\delta/2\pi = 3.0$ GHz. Thus, cold atoms can be trapped in the vicinity of the center of two pairs of metallic wedges in the x–y plane and guided in the z direction.

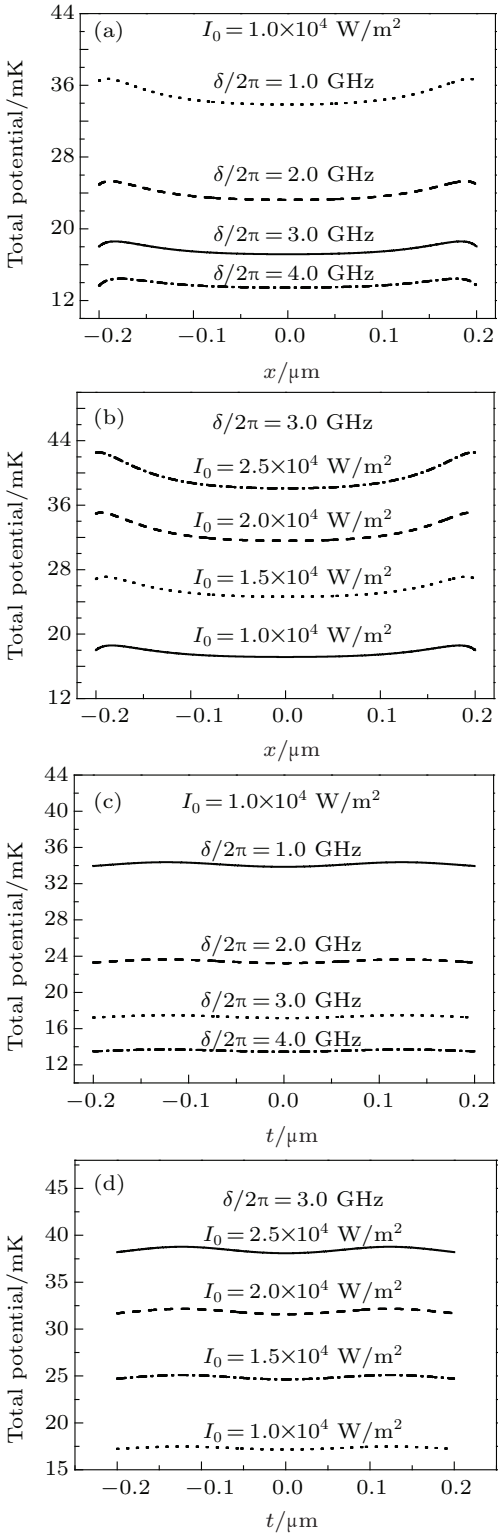


Fig. 9. 1D distribution of total potential with $d = 0.25$ μm (a) versus x as $I_0 = 1.0 \times 10^4$ W/m^2 for different $\delta/2\pi$; (b) versus x as $\delta/2\pi = 3.0$ GHz for different I_0; (c) versus t (the diagonal distance from 0 when $y = x$) as $I_0 = 1.0 \times 10^4$ W/m^2 for different $\delta/2\pi$; (d) versus t as $\delta/2\pi = 3.0$ GHz for different I_0.

On the other hand, when the atom moves in the light field, it will spontaneously emit a photon or scatter a Rayleigh or Raman photon. The corresponding spontaneous-emitting rate, Rayleigh and Raman scattering rates can be estimated by[24]

$$S_{\rm spon} = \frac{\Gamma|\Omega|^2/2}{2[(\Gamma/2)^2+\delta^2]+|\Omega|^2}, \tag{4a}$$

$$S_{\rm Rayleigh} = \frac{8\pi r_0^2 I(r)}{\hbar\omega_{\rm l}}\left(\frac{\omega_{\rm l}}{\omega_{\rm a}}\right)^4, \tag{4b}$$

$$S_{\rm Raman} = \frac{8}{9}\left(\frac{\Delta_{\rm fs}\omega_{\rm l}}{\omega_{\rm a}^2}\right)^2 S_{\rm Rayleigh}, \tag{4c}$$

where $r_0 = 2.818\times10^{-15}$ m is the classical radius of an electron, $\Delta_{\rm fs}$ is the frequency splitting of atomic fine structure, $\omega_{\rm l}$ is laser angular frequency, and $\omega_{\rm a}$ is the atomic resonant angular frequency. For ^{87}Rb-D_2 line atoms, $\omega_{\rm a}/2\pi = 3.846\times10^{14}$ Hz, and $\Delta_{\rm fs}/2\pi = 7.26\times10^{12}$ Hz. Taking $\delta/2\pi = 3.0$ GHz, $d = 0.25$ μm , and $I_0 = 1.0\times10^3$ W/m^2, for one pair of metallic wedge tips, according to Eq. (4), the spontaneous-emitting rate, Rayleigh and Raman scattering rates are 2.5×10^3, 1.7×10^{-5}, and 5.5×10^{-9} s^{-1} in the vicinity of groove of the nanoscale guiding region, respectively, and 1.9×10^3, 1.3×10^{-5}, and 4.2×10^{-9} s^{-1} in the vicinity of the center of two pairs of metallic wedge tips, respectively. It is obvious that Rayleigh and Raman scattering rates are very small and can be neglectable. However, the spontaneous-emitting rate is so large that it is not useful for guiding cold atoms. Fortunately, according to Eq. (1), we know that the intensity distribution is almost exponential, and in the gravito-optical trap (see Figs. 7(b)–7(d)), the average intensity gradient in the y direction can reach 4.5×10^{12}, 4.0×10^{10}, and 2.0×10^{11} W/m^3, respectively. In dark nanoscale trap, as shown in Fig. 8, the average intensity gradient can reach 1.1×10^{13} W/m^3. Therefore, the intensity gradients in the gravito-optical trap and the dark nanoscale trap are even larger than or similar to that of the evanescent-wave surface trap (the maximum intensity gradient is 9.7×10^{11} W/m^3) used in Ref. [25]. Therefore, the intensity gradient cooling of atoms in our nanoscale guiding region will be the same efficient as that of the evanescent-wave surface trap. Considering the intensity-gradient cooling, the spontaneous-emitting heating as well as the recoil-induced heating from the absorption of photons, we can use an equation to estimate the final equilibrium rms momentum $p_{\rm rms}$ of atoms in our nanoscale trap[26,27]

$$-\frac{1}{3}\frac{\delta_{\rm hfs}}{\delta+\delta_{\rm hfs}}\left(\frac{p_{\rm rms}}{\hbar k}\right)^2 + \frac{1}{q_r^2} + \frac{1}{1-q_i} = 0. \tag{5}$$

For an ^{87}Rb atom, $\delta_{\rm hfs}/2\pi = 6.835$ GHz, $q_i = 0.75$, and $q_r = 0.58$. From Eq. (2), we can obtain a final equilibrium rms momentum $p_{\rm rms} \approx 5.49\hbar$k as $\delta/2\pi$ =3.0 GHz, corresponding to a temperature of $T \approx 3.64$ μK. It means that the spontaneous-emitting heating can be completely balanced by the intensity-gradient cooling, and then atoms can reach a final equilibrium temperature.

4. Conclusion

In conclusion, we have proposed a novel scheme to generate two kinds of nanoscale optical fields for guiding cold atoms by using one pair and two pairs of tips of metallic wedges. We have investigated the intensity distribution near the tip of a metallic wedge, and studied the total intensity and the total potential of optical potentials and van der Waals potentials of ^{87}Rb atoms of one pair and two pairs of tips of metallic wedges. It has been found that the total potential can form a gravito-optical trap by one pair of tips of metallic wedges, and a dark nanoscale trap by two pairs of tips of metallic wedges. The dark trapping section can guide cold atoms with position uncertainties of about 130 nm, which can form a hybrid system integrating isolated atoms with solid devices. Due to the high intensity gradient in the dark nanoscale guiding region with blue-detuning, atoms can be cooled to several μK with efficient intensity-gradient Sisyphus cooling.

References

[1] Yin J, Gao W and Zhu Y 2003 *Prog. Opt.* **45** 119
[2] Xu X, Kim K, Jhe W and Kwon N 2001 *Phys. Rev. A* **63** 063401
[3] Pruvost L, Marescaux D, Houde O and Duong H T 1999 *Opt. Commun.* **166** 199
[4] Wolschrijn B T, Cornelussen R A, Spreeuw R J C and van den Heuvell H B 2002 *New J. Phys.* **4** 69
[5] Ol'Shanii M A, Ovchinnikov Yu B and Letkhov V S 1993 *Opt. Commun.* **98** 77
[6] Renn M J, Montgomery D, Vdovin O, Anderson D Z, Wieman C E and Cornell E A 1995 *Phys. Rev. Lett.* **75** 3253
[7] Renn M J, Zozulya A A, Donley E A, Cornell E A and Anderson D Z 1997 *Phys. Rev. A* **55** 3684
[8] Ito H, Nakata T, Sakaki K, Ohtsu M, Lee K I and Jhe W 1996 *Phys. Rev. Lett.* **76** 4500
[9] Wang Z, Dai M and Yin J 2005 *Opt. Express* **13** 8406
[10] Wang Z and Yin J 2006 *Opt. Express* **14** 9551
[11] Monroe C and Lukin M D 2008 *Phys. World* **21** 32
[12] Treutlein P, Steinmetz T, Colombe Y, Lev B, Hommelhoff P, Reichel J, Greiner M, Mandel O, Widera A, Rom T, Bloch I and Hansch T W 2006 *Fortschr. Phys.* **54** 702
[13] Andre A, Demille D, Doyle J M, Lukin M D, Maxwell S E, Rable P, Schoelkopf R J and Zoller P 2006 *Nature Phys.* **2** 636
[14] Folman R, Kruger P, Schmiedmayer, Denschlag J and Henkel C 2002 *Adv. At. Mol. Opt. Phys.* **48** 263
[15] Chang D E, Thompson J D, Park H, Vuletic V, Zibrov A S, Zoller P and Lukin M D 2009 *Phys. Rev. Lett.* **103** 123004
[16] Balykin V I, Klimov V V and Letokhov V S 2003 *JETP Lett.* **78** 8
[17] Klimov V V, Sekatskii S K and Dietler G 2006 *Opt. Commun.* **259** 883
[18] Chang D E, S?rensen A S, Hemmer P R and Lukin M D 2007 *Phys. Rev. B* **76** 035420
[19] Murphy B and Hau L V 2009 *Phys. Rev. Lett.* **102** 033003
[20] Stehle C, Bender H, Zimmermann C, Kern D, Fleischer M and Slama S 2011 *Nature Photon.* **5** 494
[21] Juan M L, Righini M and Quidant R 2011 *Nature Photon.* **5** 349
[22] Shaffer J P 2011 *Nature Photon.* **5** 451
[23] Yin J 2006 *Phys. Rep.* **430** 1
[24] Takekoshi T and Knize R J 1996 *Opt. Lett.* **21** 77
[25] Ovchinnikov Yu B, Manek L and Grimm R 1997 *Phys. Rev. Lett.* **79** 2225
[26] Wang Z, Cao G and Yin J 2008 *Opt. Commun.* **281** 4348
[27] Yin J and Gao W 2004 *Acta Phys. Sin.* **53** 4157 (in Chinese)